narra j

**Original Article**

# In silico studies on quercetin, myricetin, and kaempferol in inhibiting TGF-β1 and galectin-3 for cardiac fibrosis management

**Suryono Suryono[1,2*], Muhammad I. Amien[3], Achmad I. Tohari[3], Antonius D. Saputra[3], Muhammad RF. Hidayat[3] and Hazbina F. Ramadhan[4]**

[1]Department of Cardiology and Vascular Medicine, Faculty of Medicine, Universitas Jember, Jember, Indonesia; [2]Department of Cardiology and Vascular Medicine, Dr. Soebandi General Hospital, Jember, Indonesia; [3]Faculty of Medicine, Universitas Jember, Jember, Indonesia; [4]Bina Sehat Hospital, Jember, Indonesia

*Corresponding author: suryonofiha@gmail.com

## Abstract

Cardiac fibrosis remains as the leading cause of death worldwide and is often associated with elevated levels of transforming growth factor-β 1 (TGF-β1) and galectin-3, making them potential therapeutic targets. Recent studies revealed that quercetin, myricetin, and kaempferol have the biological effect for several cardiovascular diseases. However, the investigation into this topic through molecular models and analysis remain unexplored. The aim of this study was to evaluate the potential effect of quercetin, myricetin, and kaempferol which targeted TGF-β1 and galectin-3. In this study, quercetin, myricetin, and kaempferol roled as the tested ligands. Subsequently, colchicine and native ligand acted as control ligands that were screened through molecular docking against TGF-β1 and galectin-3 using AutoDock tools to identify the potential inhibitor. The stability of ligand-receptor complexes was assessed through molecular dynamic (MD) simulations using NMAD. Absorption, Distribution, Metabolism, Excretion and toxicity (ADMET) prediction were also performed using ADMETlab 2.0. Molecular docking analysis revealed that quercetin, myricetin, and kaempferol exhibited strong binding affinity which are -8.9 kcal/mol, -8.5 kcal/mol, -7.6 kcal/mol respectively with TGF-β1, and -7.5 kcal/mol, -7.0 kcal/mol, -5.7 kcal/mol respectively with galetcin-3; low inhibition constant (Ki); and stable interaction with the active sites of TGF-β1 and galectin-3. MD simulations confirmed the stability and compactness of the ligand-receptor complexes. ADMET analysis also showed high Plasma Protein Binding (PPB) values (quercetin: 95%, myricetin: 92%, and kaempferol: 97%) and moderate clearance values (quercetin: 8.284%, myricetin, and 7.716%, kaempferol: 6.868%) for the tested compounds. In conclusion, the in silico analyses suggested that quercetin, myricetin, and kaempferol are promising for cardiac fibrosis therapies by inhibiting TGF-β1 and galectin-3.

**Keywords**: Cardiac fibrosis, in silico, natural compound, TGF-β1, galectin-3

## Introduction

Cardiac fibrosis is a pathological condition characterized by the expansion of cardiac interstitial space due to the deposition of extracellular matrix proteins and fibrotic changes in the myocardium [1-3]. Several underlying conditions contribute to cardiac fibrosis, such as infections, inflammatory conditions, and metabolic disease [4]. These conditions activate the transforming growth factor-β1 (TGF-β1)-Sma- and Mad-related proteins 2/3 (Smad2/3) and galectin-3 signaling pathway [5-10]. TGF-β1 plays a pivotal role in some heart diseases such as



Received: August 10, 2024 - Accepted: December 4, 2024 - Published online: January 8, 2025

myocardial infarction [11,12] and also cardiac fibrosis [13]. In cardiac fibrosis, TGF-β1 isoforms function with activins to stimulate intracell signalling through Smad2/3 transcription factors [14]. Therefore, TGF-β1 is a promising therapeutic target for cardiac fibrosis [15]. Similarly, galectin-3 upregulates calcium-activated potassium channels ($K_{ca}3.1$) channel that could subsequently lead to cardiac fibrosis [16]. When the Kca3.1 channel is activated, it contributes to an increase in intracellular calcium levels. This activation allows $Ca^{2+}$ ions to enter the cell via channels like the transient receptor potential vanilloid 4 (TRPV4). Elevated intracellular $Ca^{2+}$ levels can contribute to cardiac fibrosis by promoting the differentiation of ventricular fibroblasts into myofibroblasts, which are involved in the fibrotic process through extracellular matrix deposition [17]. Recent studies have reported an increase in galectin-3 expression in cardiac fibrosis that was observed through in vivo and in vitro models [17-20], further supporting its potential as a therapeutic target [21].

On the other hand, recent studies revealed that quercetin, myricetin, and kaempferol which are a group of flavonoids and found in many natural plants [22-23], have the medical effect to protect against chronic diseases associated with oxidative stress, including cancer and cardiovascular disease [24-25]. We selected quercetin, myricetin, and kaempferol as ligands and TGF-β1 and galectin-3 as target proteins. structure-based virtual screening techniques were used to identify the inhibitory effect through molecular docking-, molecular dynamic simulations (RMSD, RMSF, SASA, radius of gyration), and absorption, distribution, metabolism, excretion, and toxicity (ADMET) analysis. colchicine was used as comparison ligand due to its known antifibrotic effects in cardiac fibrosis [26,27], by inhibiting TGF-β1 [28]. The aim of this study was to evaluate the potential effect of quercetin, myricetin, and kaempferol targeting TGF-β1 and galectin-3 to inhibit cardiac fibrosis through in silico analysis.

# Methods

## Selection of ligands

Three-dimensional structure of Quercetin (PubChem CID: 5280343), myricetin (PubChem CID: 5281672), and kaempferol (PubChem CID: 5280863) as the main tested ligands. Additionally, colchicine (PubChem CID: 6167) that is the native ligands served as control ligand, were selected and downloaded from PubChem (https://pubchem.ncbi.nlm.nih.gov). Based on "Lipinski's rule of five" [29], these ligands have molecular weight ≤500 Da, ≤5 hydrogen bond donor, ≤10 hydrogens bond acceptor, ≤5 Log P, and polar surface area are ≤140 Å2 that have been known from PubChem database which are determined using the Tanimoto equation and a dictionary-based binary fingerprint [30]. This indicated that these ligands have drug-like properties and good oral bioavailability. Thereafter, the downloaded files were converted from SDF format to PDB format.

## Selection of target proteins

The target proteins used in this research were TGF-β1 and galectin-3 which are elevated and become the essential pathological proteins in cardiac fibrosis based on recent studies [5-10]. The catalytic domain of TGF-β1 in complex with natural inhibitor (PDB: 3TZM) and crystal structure of galectin-3 in complex with inhibitor (PDB: 2XG3) were downloaded from the Research Collaboratory for Structural Bioinformatics (RCSB) Protein Data Bank (https://www.rscb.com) and saved as PDB file. The functional domains, the number, and name of amino acid residues that were present in the pocket of the active site of each target molecule were identified using BIOVIA Discovery Studio Visualizer 2021. The residues in the pocket of the active site of TGF-β1 include Ile211, Gly214, Ala230, Lys232, Leu278, Ser280, Asp281, Tyr282, His283, Lys335, Lys337, Leu340, and Asp351. As for galectin-3, the residues are Val116, Pro117, Asn143, Arg144, Arg162, Arg169, Asn174, Trp181, Glu184, Arg186, Ser188, Phe190, Ser237, Gly238, Asp239, and Ile240.

## Preparation of target proteins and ligands

Quercetin, myricetin, kaempferol, and colchicine as ligands were prepared by adjusting ionization, torsion, degree of freedom, and stereo-chemical variation using AutoDock MGL Tool.

Gasteiger charges and polar hydrogens were added, and the torsion angles were set. After that, the ligand file was saved as pdbqt format. TGF-β1 and galectin-3 as target receptors were prepared by deleting water molecules, deleting natural ligand, and identifying the amino acid residues of their active sites using BIOVIA Discovery Studio Visualizer 2021 and then adding Kollman charge and polar hydrogen bond using AutoDock tools.

## Molecular docking

Molecular docking was performed using in silico docking software AutoDock tools. Through this procedure, we analyzed the binding affinity (Kcal/mol), final intermolecular energy (Kcal/mol), inhibition constant Ki (μM), and the type of interactions. Before docking the main tested ligands, we did the docking validation of two target proteins using its native ligands. After that, quercetin, myricetin, kaempferol, and colchicine were docked one by one against TGF-β1 (PDB: 3TZM) and galectin-3 (PDB: 2XG3) by specific docking (mentioned previously). The grid box used for the docking simulation targeting TGF-β1 was 44×48×60 Å for the x, y, and z dimensions, respectively. The grid box used for the docking simulation targeting TGF-β1 had dimensions of 44×48×60 Å for the x, y, and z axes, respectively. The center of the grid box was positioned at the coordinates (3.562; 9.117; 7.001 Å) along the x, y, and z axes, respectively. For the simulation targeting galectin-3, the grid box size was set to 71×58×68 Å for the x, y, and z dimensions. The docking coordinates were centered at -13.176; 8.709; 6.976 Å along the x, y, and z axes. The docking was performed using command prompt and the other prerequisite conditions before the docking such as ligand and enzyme preparation were established. PyMol and BIOVIA Discovery Studio Visualizer were used to visualize the binding interaction between the active compounds of quercetin, myricetin, kaempferol, and colchicine with 3D structure of two target receptors.

## MD simulations

The configuration of the most negative value conformation of ligands output was combined with each receptor using BIOVIA discovery studio, added hydrogen bonds to the complexes, and saved as PDB format. The topology files and parameters of ligand-receptors complex were made using the CHARMM-GUI website (https://www.charmm-gui.org) [31]. Molecular dynamics (MD) simulations of the ligand and each receptor complex were performed using NAMD software [32]. The preparation step consists of energy minimization, equilibration, and production. The missing hydrogen atoms from the previous ligand preparation of quercetin, myricetin, kaempferol, and colchicine were added with the polar hydrogen. The systems were solvated using TIP3P water molecules and were neutralized using sodium and chloride ions (NaCl) at the ionic concentration of 0.154 M using the Monte-Carlo for ion positioning. All complexes were solvated using the transferable intermolecular potential water molecules (TIP3P) model. The CHARMM36 force field was used for 10.000 steps energy minimization by the Steepest Descent method. After that, the system was equilibrated at 310 K for 100 ns in a constant atom number, volume and temperature (NVT) ensemble. Subsequently, in a constant number of atoms, pressure, and temperature (NPT) ensemble, the system was subjected to 100 ns with the temperature and pressure were set using a reference temperature (310 K) and pressure (1 atm) respectively [33]. After that, the Root Mean Square Deviation (RMSD), Root Mean Square Fluctuation (RMSF), Solvent Accessible Surface Area (SASA), and Radius of Gyration (Rg) analysis for 100 ns were analyzed and visualized using VMD tools. Binding free energies of the complexes was also calculated by means of molecular Mechanics-Generalized-Born surface area (MM-GBSA) utilizing of Amber tools [34]. The binding free energy could be obtained through the following equations:

$$\Delta G_{bind} = G_{complex} - G_{receptor} - G_{ligand} \quad (1)$$

$$\Delta G_{bind} = \Delta H - T\Delta S \quad (2)$$

$$\Delta H = \Delta G_{gas} + \Delta G_{sol} \quad (3)$$

$$\Delta G_{gas} = E_{vdw} + E_{elec} \quad (4)$$

$$\Delta G_{sol} = E_{sol\,(gb)} + E_{np} \quad (5)$$

where the $\Delta H$, $T\Delta S$, $E_{vdw}$, $E_{elec}$, $E_{sol\ (gb)}$, and $E_{np}$ represented enthalpy change, the entropic contribution, van der Waals interaction energy, electrostatic interaction energy, the polar solvation energy (GB model) and the non-polar solvation energy, respectively. Additionally,

principal Component Analysis (PCA) based Free Energy Landscape (FEL) also performed, and then the free energy landscape of the ligands and target proteins bound was calculated and visualized using OriginLab2018 tools [35].

### ADMET properties selection

The pharmacokinetic ADMET and toxicity properties of quercetin (SMILES: C1=CC(=C(C=C1C2=C(C(=O)C3=C(C=C(C=C3O2)O)O)O)O)O); kaempferol (SMILES: C1=CC(=CC=C1C2=C(C(=O)C3=C(C=C(C=C3O2)O)O)O)O); and myricetin (SMILES: C1=C(C=C(C(=C1O)O)O)C2=C(C(=O)C3=C(C=C(C=C3O2)O)O)O) included bioavailability, human intestinal absorption, protein plasma binding, brain penetration, human hepatotoxicity, cardiac toxicity, and carcinogenicity that were determined by using ADMETlab 2.0 webserver (https://admetmesh.scbdd.com/service/evaluation/index). The good ADMET results were shown by fulfilling several criteria including met the Lipinski rule of five criteria as mentioned before, have an excellent Human Intestinal Absorption, the high value of plasma protein binding (> 90%), an excellent brain penetration, and low or moderate clearance (5–20%) [36].

## Results

### Molecular docking

#### *Docking validation*

The re-docking step was performed to examine the docking procedure, efficiencies, and validation of the target proteins. The 4-[5-(1,3-benzodioxol-5-yl)-4-(pyridin-2-yl)-1H-imidazol-2-yl] benzamide peptide inhibitor as the native ligand from TGF-β1, and benzamide peptide inhibitor as the native ligand from galectin-3 were removed and re-docked into the active site using AutoDock Vina. The peptide inhibitor bound exactly to the active site of TGF-β1 with good binding energy of −9,1 kcal/mol. Tyr282, His283, Asp351, Ile211, Gly214, Leu278, Ala230, Lys232, Ser280, and Asp281 are the interacting amino acids. The re-docked complex was then superimposed on to the native co-crystallized 4-[5-(1,3-benzodioxol-5-yl)-4-(pyridin-2-yl)-1H-imidazol-2-yl] benzamide - TGF-β1 from PDB using PyMOL and a low RMSD of 0.183 Å was observed. Meanwhile the peptide inhibitor also bound to the active site of galectin-3 with good binding energy of −8.1 kcal/mol. Val116, Asn143, Arg144, Gly238, Asp239, Pro117, Ser237, Ile240 are the interacting amino acids. RMSD value from the re-docked complex of co-crystallized benzamide – galectin-3 was also found to be low (1.355 Å) (**Figure 1**).

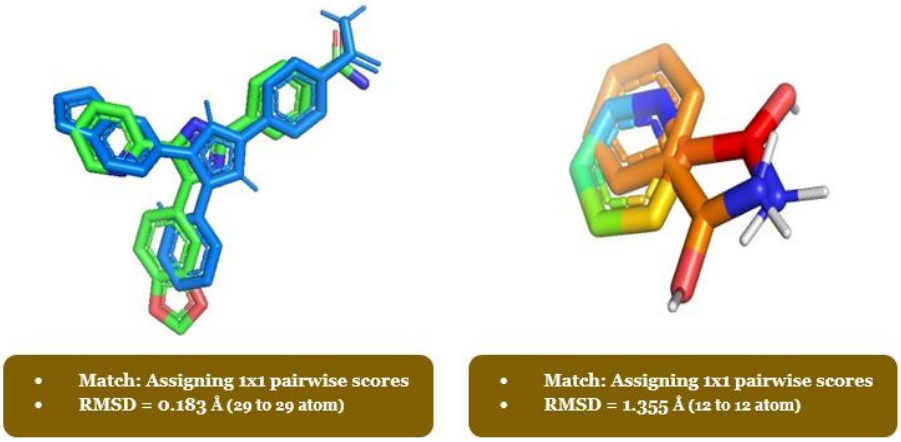


Figure 1. The docking validation of TGF-β1 (A) and galectin-3 (B) using PyMol.

#### *Ligands targeting TGF-β1*

The catalytic domain of TGF-β1 has some important amino acid residues as the active sites that are responsible for its inhibitory effect, which are Ile211, Gly214, Ala230, Lys232, Leu278, Ser280, Asp281, Tyr282, His283, Lys335, Lys337, Leu340, and Asp351. The molecular docking poses of top conformers with the most negative energy for the native ligand, quercetin, myricetin,

kaempferol, and colchicine demonstrated binding to some active sites of TGF-β1. The docking poses of the most negative energy for tested ligands also showed similarities to the pose of native ligand based on their positions and the amino acid residues they bind to TGF-β1 (**Figure 2**).

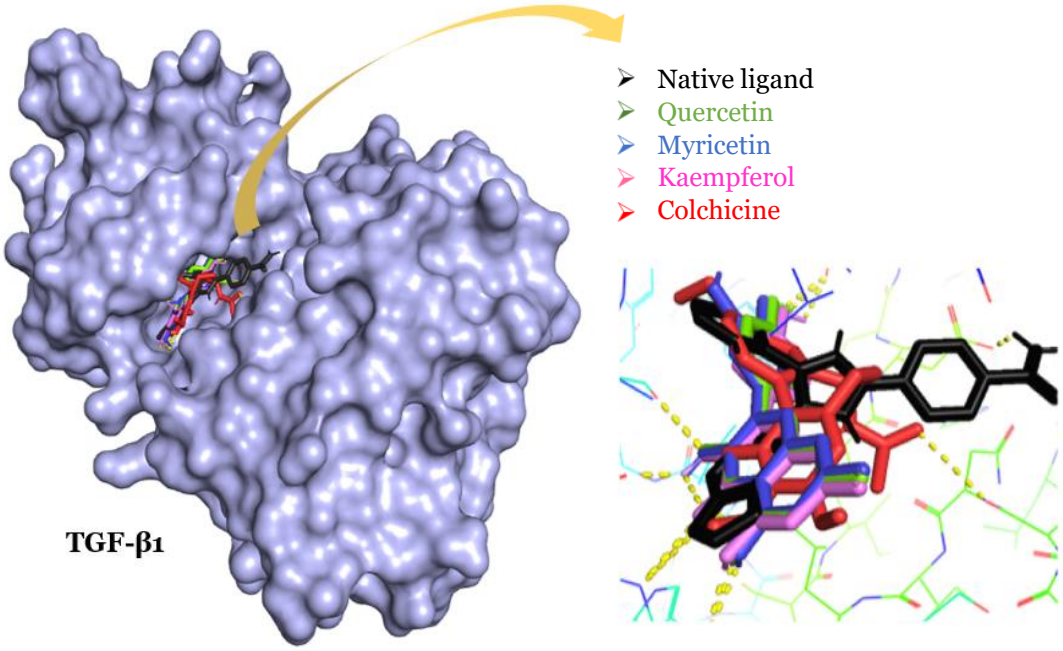


Figure 2. The docking poses of tested ligands and native ligand of TGF-β1.

The binding affinities of the main tested ligands are more negative compared to colchicine (-6.9 kcal/mol), with quercetin exhibted the most negative binding affinity (-8.9 kcal/mol). However, quercetin's binding affinity was not as negative as that of the native ligand (-9.1 kcal/mol). Quercetin has the lowest final intermolecular energy of -9.84 kcal/mol compared to other ligands and colchicine. It binds to the active sites of TGF-β1 through conventional hydrogen bond with Ile211, Ser280, Asp281, His283, and Asp351; and through Van der Wall interactions with Leu278 and Tyr282. Myricetin binds to TGF-β1 with final intermolecular energy of -9.80 kcal/mol and bound to the active sites of TGF-β1 through conventional hydrogen bond with Ile211, Ser280, Asp281, and His283; and through Van der Wall interactions with Leu278 and Asp351. Kaempferol bound to TGF-β1 with final intermolecular energy of -8.92 kcal/mol and the active sites of TGF-β1 through conventional hydrogen bond with Ile211, Lys232, Ser280, Asp281, His283, and Asp351; and through Van der Wall interaction with LEU278. Meanwhile, Colchicine bound to TGF-β1 with final intermolecular energy of -8.11 kcal/mol and the active sites of TGF-β1 through carbon hydrogen bond with Ser280 and His283 (**Figure 3**). On the other hand, the lowest inhibition constant (Ki) of native ligand, quercetin, myricetin, kaempferol, and colchicine respectively were 167.01 µM, 1.26 µM, 1.96 µM, 3.57 µM, and 4.05 µM (**Table 1**).

### *Ligands targeting galectin-3*

Galectin-3 has important amino acid residues as active sites that are responsible for its inhibitory effect, those are Val116, Pro117, Asn143, Arg144, Arg162, Arg169, Asn174, Trp181, Glu184, Arg186, Ser188, Phe190, Ser237, Gly238, Asp239, and Ile240. The molecular docking results showed the lowest binding affinity complex was quercetin (-7.5 kcal/mol). This binding affinity wass more negative than colchicine (-6.3 kcal/mol) and not more negative compared to the native ligand (-8.1 kcal/mol) (**Figure 4**). Quercetin had the lowest final intermolecular energy of -8.60 kcal/mol compared to other ligands and colchicine., and it bound to the active sites of galectin-3 through conventional hydrogen bonds with Val116, Asp239; and through Van der Wall interactions with Gly238 and Ile240. Myricetin bound to galectin-3 with final intermolecular energy of -8.18 kcal/mol and the active sites of galectin-3 through conventional hydrogen bond with Val116, Gly238, and Asp239. Kaempferol bound to galectin-3 with final intermolecular

energy of -7.22 kcal/mol with no conventional hydrogen bond and no Van der Wall interaction with the active sites of Galectin-3. Meanwhile, Colchicine is bound to galectin-3 with final intermolecular energy of -7.86 kcal/mol and the active sites of galectin-3 through conventional hydrogen bond with Pro117 (**Figure 5**). On the other hand, the lowest inhibition constant (Ki) of native ligand, quercetin, myricetin, kaempferol, and colchicine respectively were 109.12 µM, 10.24 µM, 34.31 µM, 63.11 µM, and 61.02 µM (**Table 1**).

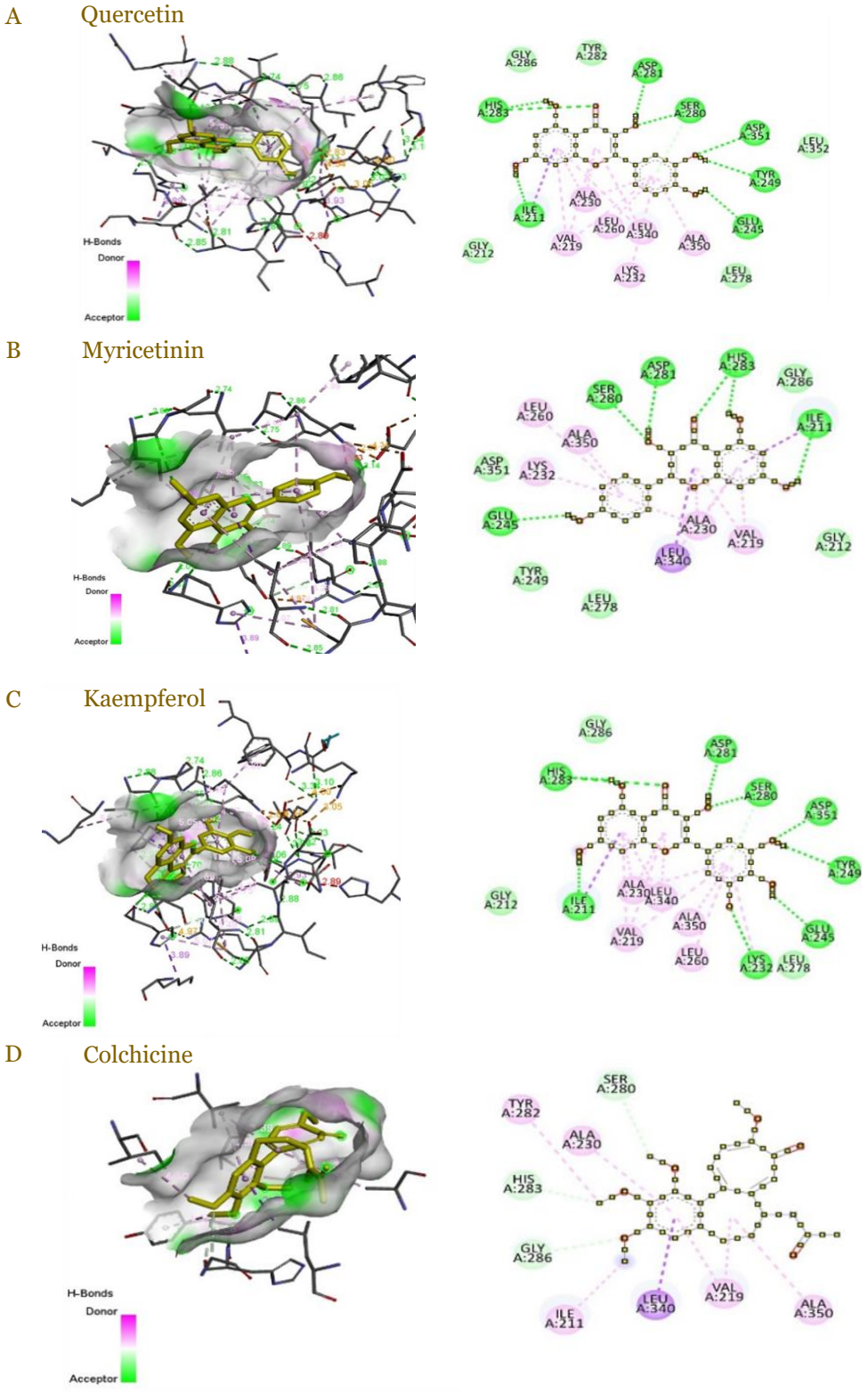


Figure 3. The interaction model of TGF-β1 with quercetin (A), myricetin (B), kaempferol (C), and colchicine (D).

Table 1. Topmost negative energy docked conformation from each ligand with target proteins

| Target protein | Ligand | Binding affinity (kcal/mol) | Final intermolecular energy (kcal/mol) | | | Inhibition constant, Ki (µM) | Interactions and involved residues |
|---|---|---|---|---|---|---|---|
| | | | vdW + Hbond + desolv energy | Electrostatic energy | Total energy | | |
| TGF-β1 (PDB: 3TZM) | Native ligand | -9.1 | -9.94 | -0.20 | -10.14 | 167.01 | Conventional Hbon: Tyr282, His283, Asp351<br>vdW: Ile211, Gly214, Leu278, Ala230, Lys232, Ser280, Asp281 |
| | Quercetin | -8.9 | -9.55 | -0.29 | -9.84 | 1.26 | Conventional Hbon: Ile211, Ser280, Asp281, His283, Asp351<br>vdW: Leu278, Tyr282 |
| | Myricetin | -8.5 | -9.60 | -0.20 | -9.80 | 1.96 | Conventional Hbon: Ile211, Ser280, Asp281, His283<br>vdW: Leu278, Asp351 |
| | Kaempferol | -7.6 | -8.76 | -0.16 | -8.92 | 3.57 | Conventional Hbon: Ile211, Lys232, Ser280, Asp281, His283, Asp351<br>vdW: Leu278 |
| | Colchicine | -6.9 | 8.0 | -0.11 | -8.11 | 4.05 | Carbon Hbon: Ser280, His283<br>vdW: - |
| Galectin-3 (PDB: 2XG3) | Native ligand | -8.1 | -8.9 | -0.35 | -9.25 | 109.12 | Conventional Hbon: Val116, Asn143, Arg144, Gly238, Asp239<br>vdW: Pro117, Ser237, Ile240 |
| | Quercetin | -7.5 | -7.79 | -0.81 | -8.60 | 10.24 | Conventional Hbon: Val116, Asp239<br>vdW: Gly238, Ile240 |
| | Myricetin | -7.0 | -7.57 | -0.61 | -8.18 | 34.31 | Conventional Hbon: Val116, Gly238, Asp239<br>vdW: - |
| | Kaempferol | -5.7 | -6.97 | -0.25 | -7.22 | 63.11 | Conventional Hbon: -<br>vdW: - |
| | Colchicine | -6.3 | -7.85 | -0.01 | -7.86 | 61.02 | Conventional Hbon: Pro117<br>vdW: - |

Hbond: Hydrogen bond; vdW: van der Waals; Desolv energy: Desolvation energy

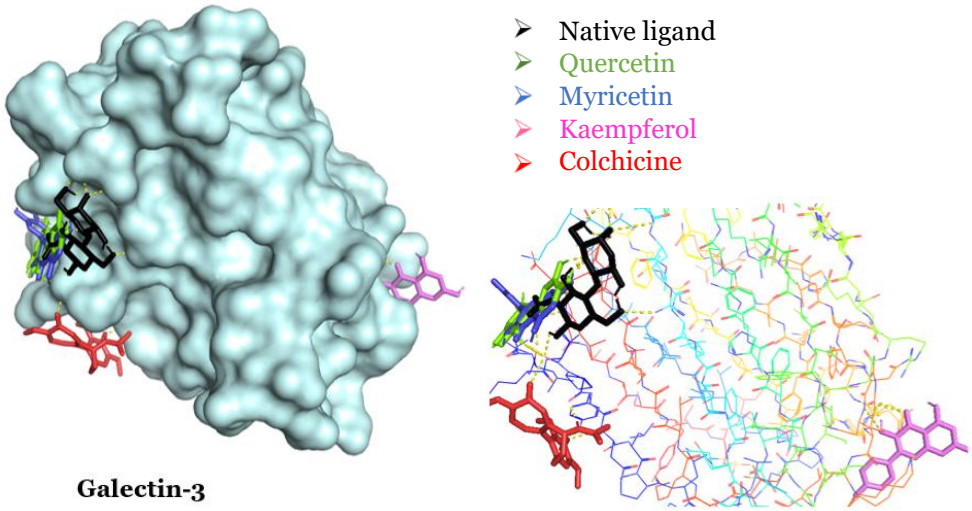


Figure 4. The docking poses of tested ligands and native ligand of galectin-3.

## Molecular dynamic simulation

The RMSD for the complex of TGF-β1 and the ligands showed a steady state with a fewer change after 30 ns observation from the total simulation period of 100 ns with the average RMSD value of 0.124 nm (1.24 Å), 0.132 nm (1.32 Å), 0.150 nm (1.50 Å), 0.154 nm (1.54 Å), 0.171 nm (1.71 Å) for native ligand, quercetin, myricetin, kaempferol, and colchicine respectively that denoted fewer changes in the overall structure during the simulation time. Quercetin as tested ligand displayed the most stable simulation system with the lowest average RMSD value of 1.32 Å among other tested ligands, and comparison ligand. The mean RMSF value of native ligand, quercetin, myricetin, kaempferol, and colchicine at the active sites of TGF-β1 respectively were 0.102 nm (1.02 Å), 0.122 nm (1.22 Å); 0.128 nm (1.28 Å); 0.136 nm (1.36 Å) and 0.151 nm (1.51 Å). From the results, there were fewer fluctuation for the complex of quercetin, myricetin, and kaempferol as tested ligands at residues Leu278, Ser280, Asp281, Tyr282, and His283 of TGF-β1 than colchicine as comparison ligand. Based on RMSF value, the most stable tested ligand with the least fluctuation is quercetin followed by myricetin and kaempferol for TGF-β1 target protein. Through Rg simulation, the complex of native ligand, quercetin, myricetin, kaempferol, and colchicine with TGF-β1 have steady average Rg of 2.21 nm, 2.40 nm, 2.65 nm, 2.41 nm, and 2.43 nm respectively over 100 ns MD simulation, indicating that quercetin is the most compact and stable for tested ligand due to its lower Rg value than other tested ligands, followed by kaempferol and myricetin. SASA maximal values of native ligand, quercetin, myricetin, kaempferol, and colchicine with TGF-β1 respectively were 146 $nm^2$, 145.7 $nm^2$, 147.1 $nm^2$, 147.9 $nm^2$ and 148.6 $nm^2$ (**Figure 6**).

For galectin-3 receptor, the average RMSD value of native ligand, quercetin, myricetin, kaempferol, and colchicine respectively were 0.172 nm (1.72 Å), 0.211 nm (2.11 Å), 0.195 nm (1.95 Å), 0.234 nm (2.34 Å), 0.231 nm (2.31 Å), which were observed with fewer change after 40 ns of simulation. Myricetin displayed the most stable simulation system with the lowest average RMSD value of 1.95 Å among other tested ligands and comparison ligand. The mean RMSF value were 0.091 nm (0.91 Å), 0.113 nm (1.13 Å); 0.134 nm (1.34 Å); 0.152 nm (1.52 Å) and 0.144 nm (1.44 Å) for native ligand, quercetin, myricetin, kaempferol, and colchicine respectively at the active sites of galectin-3. From the results, there were minor fluctuation for the complex of quercetin and myricetin as tested ligands at residues VAL116 and PRO117 of galectin-3 than kaempferol as tested ligand and colchicine as comparison ligand. Based on RMSF value, the most stable tested ligand with the least fluctuation is quercetin followed by myricetin and kaempferol for galectin-3 target protein. The complex of native ligand, quercetin, myricetin, kaempferol, and colchicine with galectin-3 have steady average Rg of 3.12 nm, 3.41 nm, 3.51 nm, 3.37 nm, and 3.35 nm respectively over 100 ns MD simulation, indicating that kaempferol is the most stable for tested ligand through Rg simulation, followed by quercetin and myricetin, while colchicine showed the lower value than all tested ligands. SASA maximal values of native ligand, quercetin, myricetin,

kaempferol, and colchicine with TGF-β1 respectively were 148 nm², 147 nm², 146.6 nm², 148.1 nm² and 148.7 nm². Overall, myricetin from tested ligand had lower SASA which indicted it can make a compact and stable bond with TGF-β1, followed by quercetin and kaempferol as tested ligands, then colchicine as comparison ligand (**Figure 7**). The overall results of MD simulation can be seen in **Table 2**.

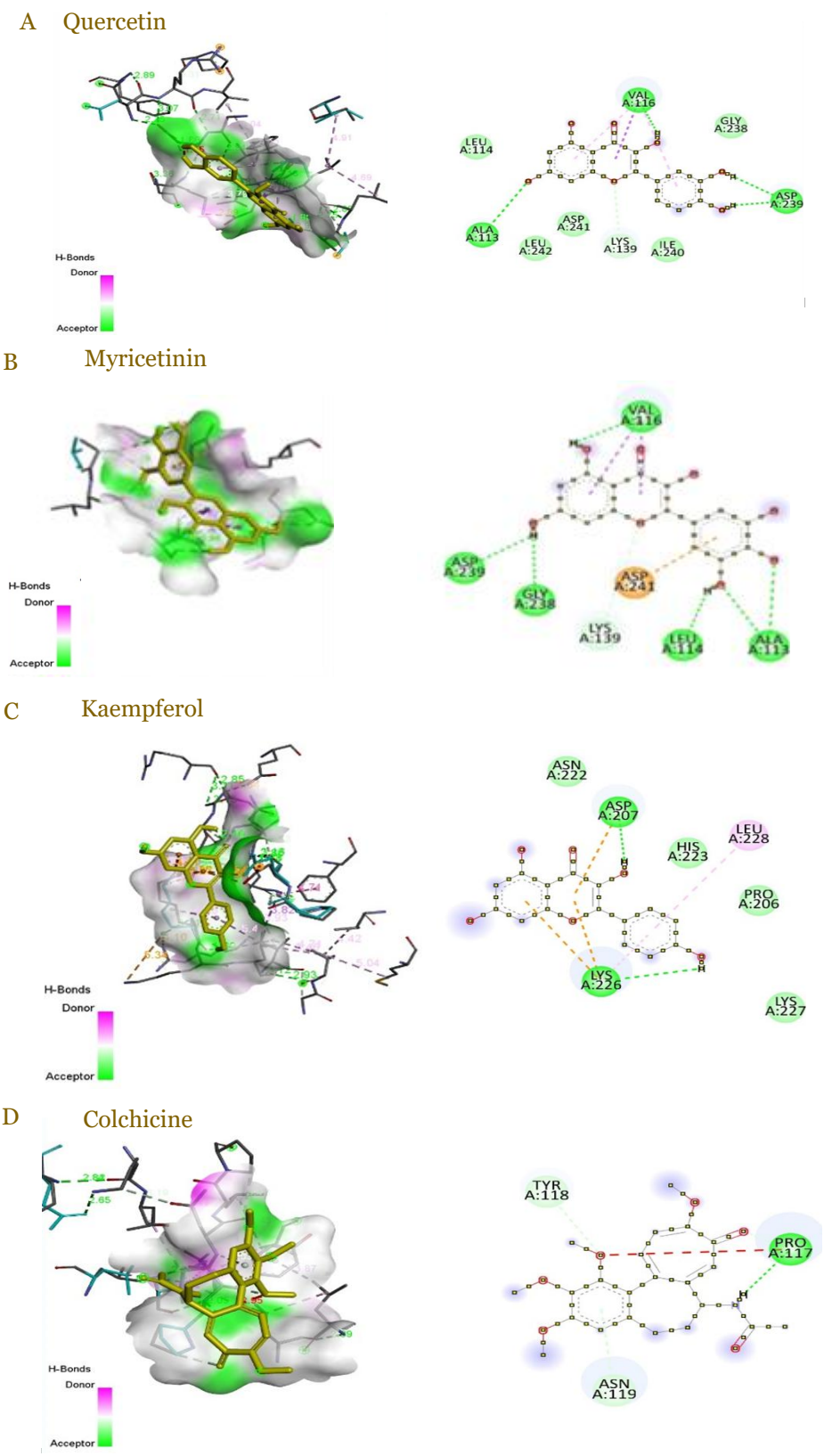


Figure 5. The interaction model of galectin-3 with quercetin (A), myricetin (B), kaempferol (C), and colchicine (D).

Table 2. The RMSD, RMSF, Rg, and SASA values for simulation trajectories throughout 100 ns of production runs

| Receptor-ligand complex | RMSD | RMSF | Rg | SASA |
|---|---|---|---|---|
| | Mean (nm) | Mean (nm) | Mean (nm) | Max (nm²) |
| TGF-β1 | 0.124 | 0.102 | 2.21 | 146 |
| Quercetin-TGF-β1 | 0.132 | 0.122 | 2.40 | 145.7 |
| Kaempferol-TGF-β1 | 0.150 | 0.128 | 2.65 | 147.1 |
| Myricetin-TGF-β1 | 0.154 | 0.136 | 2.41 | 147.9 |
| Colchicine-TGF-β1 | 0.171 | 0.151 | 2.43 | 148.6 |
| Galectin-3 | 0.172 | 0.091 | 3.12 | 148 |
| Quercetin-galectin-3 | 0.211 | 0.113 | 3.41 | 147 |
| Kaempferol-galectin-3 | 0.195 | 0.134 | 3.51 | 146.6 |
| Myricetin-galectin-3 | 0.234 | 0.152 | 3.37 | 148.1 |
| Colchicine-galectin-3 | 0.231 | 0.144 | 3.35 | 148.7 |

RMSD: root mean square deviation; RMSF: root mean square fluctuation; Rg: radius of gyration; SASA: solvent accessible surface area

The binding free energy through MMGBSA values represented in **Table 3**. The results were correlated with the binding affinity score to identify drug-like potent inhibitors. The most negative MMGBSA value indicated a stronger binding affinity between the ligand and the receptor. Based on MMGBSA, quercetin is the best tested ligand for both TGF-β1 and galectin-3 with the lowest value of -51.31±5.24 and -36.43±3.66 respectively.

Table 3. Binding free energy of the ligands with TGF-β1 or galectin-3

| Receptor-ligand complex | $E_{vdw}$ (L² atm/mol²) | $E_{ele}$ (J) | $E_{sol(gb)}$ (kcal/mol.nm²) | $E_{np}$ (kcal/mol.nm²) | $\Delta G_{bind(gb)}$ (kcal/mol) |
|---|---|---|---|---|---|
| Quercetin-TGF-β1 | -41.50±4.57 | -31.59±6.05 | 25.85±4.85 | -4.73±0.37 | -51.31±5.24 |
| Kaempferol-TGF-β1 | -31.10±4.06 | -13.82±4.07 | 9.49±4.10 | -2.63±0.30 | -37.11±3.93 |
| Myricetin-TGF-β1 | -44.37±3.96 | -21.95±5.59 | 21.31±6.01 | -4.48±0.27 | -48.30±4.75 |
| Colchicine-TGF-β1 | -24.31±4.15 | -23.01±6.17 | 28.34±4.96 | -2.80±0.39 | -21.78±4.62 |
| Quercetin-galectin-3 | -2613±4.93 | -26.60±2.73 | 19.13±4.26 | -2.90±0.25 | -36.43±3.66 |
| Kaempferol-galectin-3 | -30.45±3.14 | -30.09±7.18 | 33.85±8.92 | -2.02±0.30 | -28.65±3.62 |
| Myricetin-galectin-3 | -32.34±9.07 | -33.27±4.26 | 37.56±8.41 | -4.86±0.40 | -33.22±5.40 |
| Colchicine-galectin-3 | -25.67±6.21 | -24.33±6.23 | 29.71±5.46 | -2.76±0.46 | -23.05±3.50 |

$E_{vdw}$: van der Waals interaction energy; $E_{elec}$: electrostatic interaction energy; $E_{sol\ (gb)}$: polar solvation energy (GB model); and $E_{np}$: non-polar solvation energy; $\Delta G_{bind(gb)}$: binding free energy (GB model)

Additionally, the free-energy landscape (FEL) was investigated against the radius of gyration (Rg) and the root-mean square deviation (RMSD) as the two reaction coordinates to depict the energy minima landscape of lead complexes. It has been performed to describe conformational changes associated with protein folding and unfolding processes. All ligands with target proteins presented a funnel-like shape (**Figure 8**). The lower Gibbs free energy conformational states were shown by the deeper purple. Meanwhile, the narrow energy basin indicated the low stability of structural conformation, and the large energy basin show the high stability. The complex of quercetin-TGF-β1 and quercetin-galectin-3 showed the large energy basin with multiple global energy minima with purple color. Complex of myricetin-TGF-β1, kaempferol-TGF-β1, myricetin-galectin-3, and kaempferol-galectin-3 showed the large single global energy minima. On the other hand, the complex of colchicine-TGF-β1 and colchicine-galectin-3 as control ligand showed the narrower energy basin than the tested ligands with single energy minima. Based on the FEL analysis, quercetin is the best ligand for both TGF-β1 and galectin-3.

## ADMET prediction

ADMET analysis showed that quercetin, myricetin, and kaempferol met the specifications in Lipinski rules, so these three agents could be potential as ligands for the target protein in docking models and MD simulation. In the absorption profile, these ligands had excellent absorption profile especially through human intestinal absorption, and also not act as neither Pgp-inhibitor nor Pgp-substrate. Based on the distribution profile (**Table 4**), the Plasma Protein Binding (PPB) scores of quercetin, myricetin, and kaempferol, respectively, were 95%, 92%, and 97%, which were categorized as high (>90%). The high values of PPB indicated the low therapeutic index and

probably leading to toxicity, because of the large amounts of drugs bound to plasma protein and fewer drugs which are free that could give the effect on the target cells.

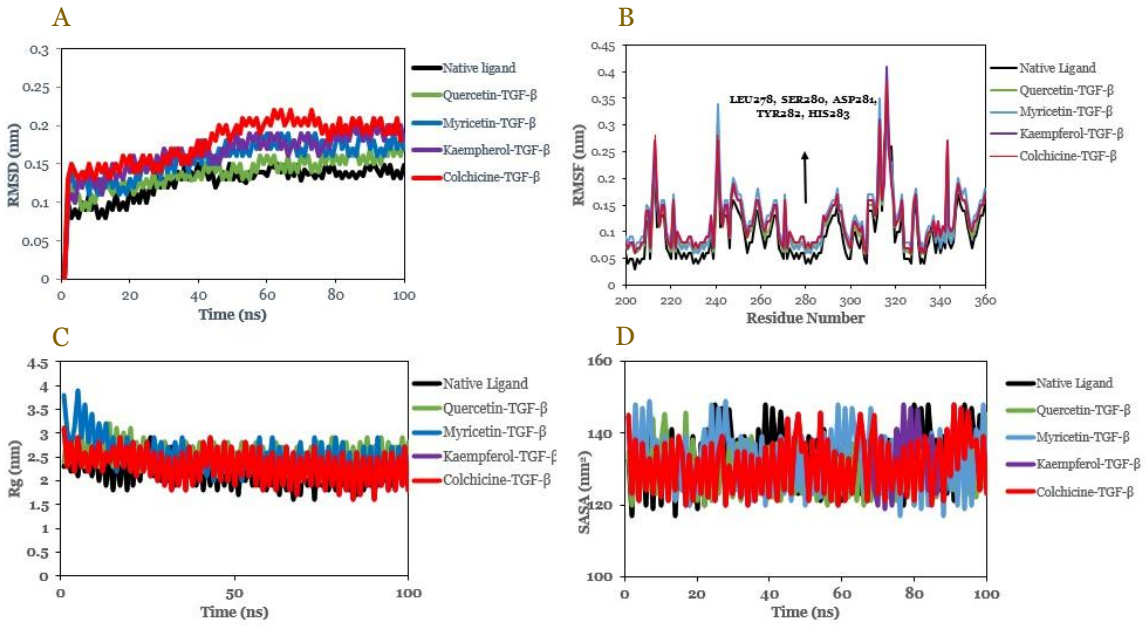


Figure 6. The RMSD (A), RMSF (B), Rg (C), and SASA (D) plot of the ligands with TGF-β1.

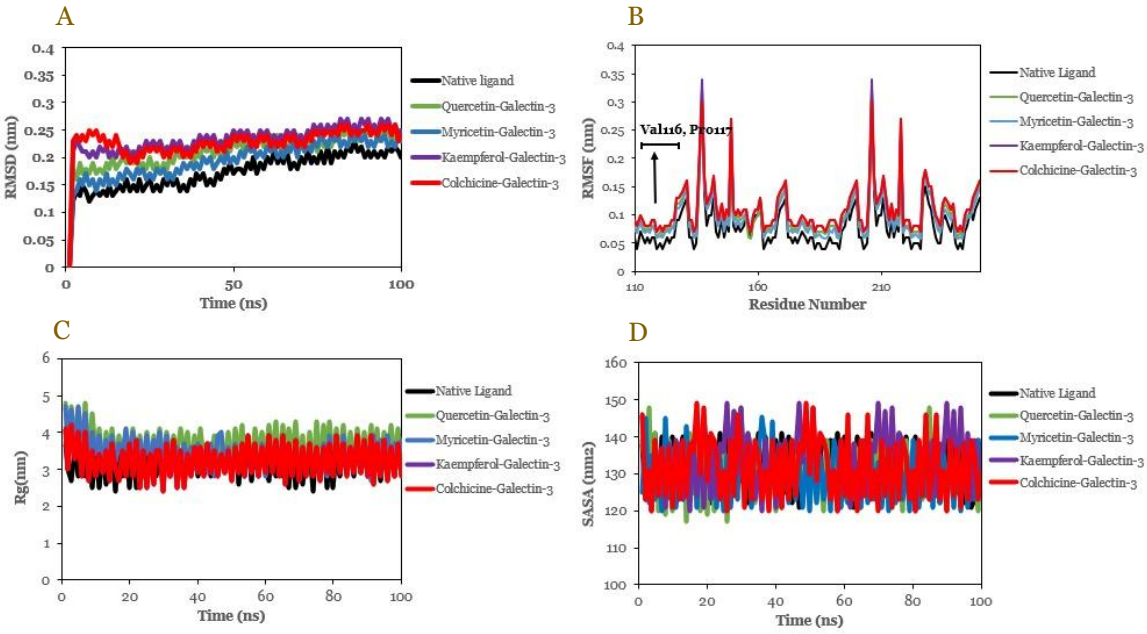


Figure 7. The RMSD (A), RMSF (B), Rg (C), and SASA (D) plot of the ligands with galectin-3.

On the other hand, based on analysis from the fraction of unbound (FU) drugs in plasma, quercetin and myricetin have 7.423% and 10.346% FU's score respectively, which were categorized medium (5–20%). The medium FU score indicated that there was a sufficient amount of free quercetin and myricetin in plasma. Therefore, despite their high PPB scores, the therapeutic index of these two ligands remained favorable. Based on excretion profile, the clearance scores of quercetin, myricetin, and kaempferol respectively were 8.284; 7.716; and 6.868 which are categorized moderate. The moderate clearance meant that these ligands were neither excessively nor insufficiently excreted through the renal system, indicating a lower toxicity profile for these ligands. Finally, based on toxicity profile these ligands are non-carcinogenic, exhibit low hepatotoxicity and low cardiac toxicity by not blocking the human

Ether-à-go-go-Related Gene (h-ERG) gene which would induce undesired lethal arrhythmia (**Table 4**).

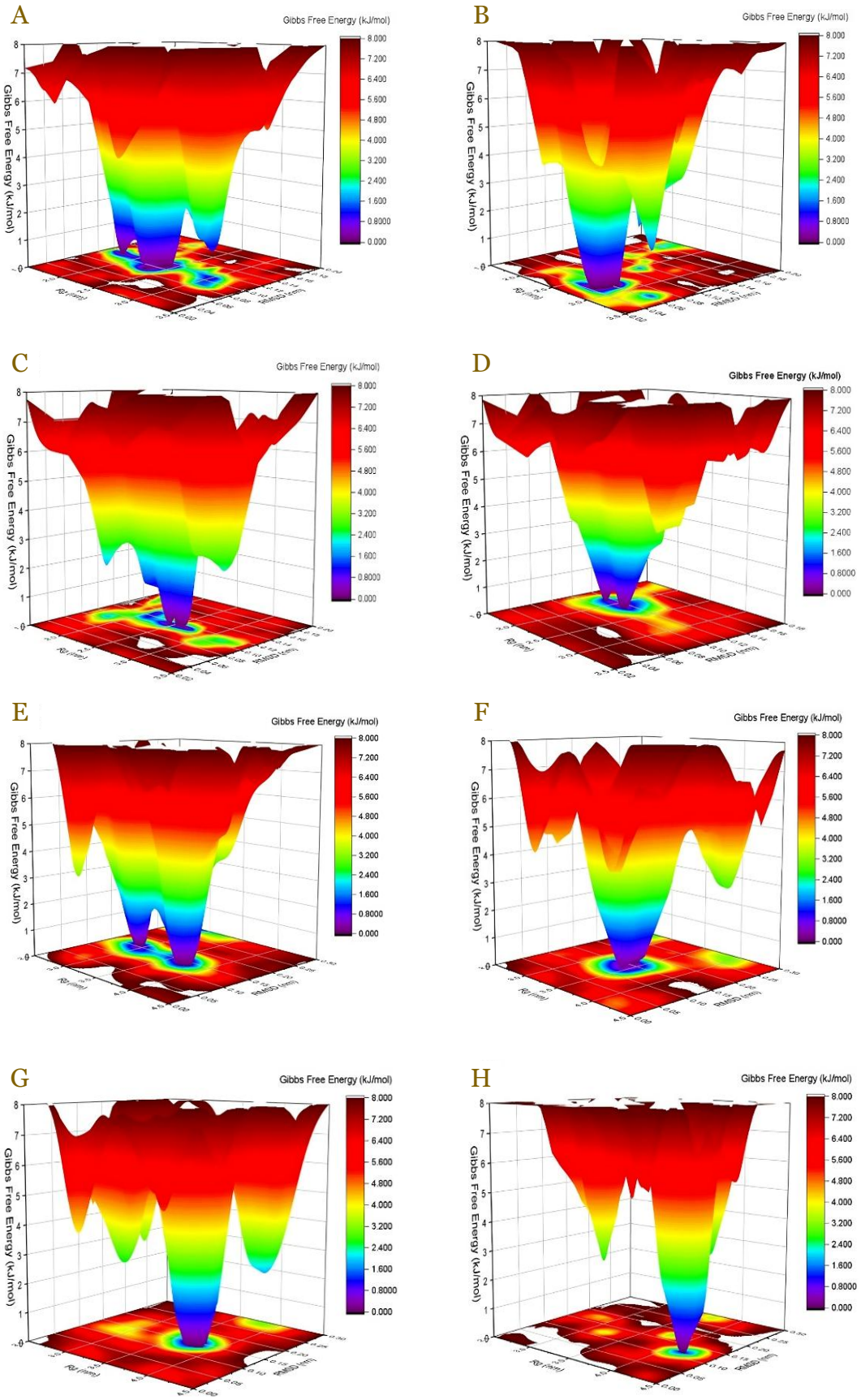


Figure 8. Free energy landscape of quercetin-TGF-β1 (A), myricetin-TGF-β1 (B), kaempferol-TGF-β1 (C), colchicine-TGF-β1 (D); and quercetin-galectin-3 (E), myricetin-galectin-3 (F), kaempferol-galectin-3 (G), colchicine-galectin-3 (H).

Table 4. Ligands physicochemical and ADMET properties of quercetin, myricetin, and kaempferol

| ADMET properties | Quercetin | | Myricetin | | Kaempferol | |
|---|---|---|---|---|---|---|
| | Value | Remark | Value | Remark | Value | Remark |
| Physicochemical | | | | | | |
| Molecular weight | 302.040 g/mol | Proper | 318.230 g/mol | Proper | 286.240 g/mol | Proper |
| A Log P | 2.155 | Optimal | 1.747 | Optimal | 2.656 | Optimal |
| Hydrogen bond | 5 | Optimal | 6 | Optimal | 4 | Optimal |
| Hydrogen acceptor | 7 | Optimal | 8 | Optimal | 6 | Optimal |
| Lipinski rules | NA | Accepted | NA | Accepted | NA | Accepted |
| Absorption | | | | | | |
| Human intestinal absorption | ≥30% | Excellent | ≥30% | Excellent | ≥30% | Excellent |
| P-gp-inhibitor | Nil | Non-inhibitor | Nil | Non-inhibitor | Nil | Non-inhibitor |
| P-gp-substrate | Nil | Non-substrate | Nil | Non-substrate | Nil | Non-substrate |
| Distribution | | | | | | |
| Plasma protein binding | 95% | High | 92% | High | 97% | High |
| Fraction Unbound in Plasma | 7.423% | Medium | 10.346% | Medium | 4.412% | Low |
| Brain Penetration | Nil | Excellent | Nil | Excellent | Nil | Excellent |
| Metabolism | | | | | | |
| CYP2C19-inhibitor | Nil | Non-inhibitor | Nil | Non-inhibitor | Nil | Non-inhibitor |
| CYP2C19-substrate | Nil | Non-substrate | Nil | Non-substrate | Nil | Non-substrate |
| Excretion | | | | | | |
| Clearance | 8.284 | Moderate | 7.716 | Moderate | 6.868 | Moderate |
| Toxicity | | | | | | |
| Hepatotoxicity | Nil | Non-toxic | Nil | Non-toxic | Nil | Non-toxic |
| Carcinogenicit | Nil | Non-cardiogenic | Nil | Non-cardiogenic | Nil | Non-cardiogenic |
| h-ERG BlOCKERS | Nil | Inactive | Nil | Inactive | Nil | Inactive |

NA: not applicable

## Discussion

Molecular docking analysis of all three tested ligands showed favorable potential as inhibitor for both of TGF-β1 and galectin-3 through binding affinity, final intermolecular energy, and inhibition constant (Ki) parameters. The more negative binding affinity, final intermolecular energy, and inhibition constant (Ki), the easier of ligands to bind with the target protein [39,40]. Based on binding affinity and final intermolecular energy observed in the present study, the best ligand for TGF-β1 is quercetin, followed by myricetin and kaempferol as tested ligands. Based on inhibition constant, the best inhibitor for tested ligand is quercetin, followed by myricetin, kaempferol, and colchicine as comparison ligand. For galectin-3 receptor, based on binding affinity and final intermolecular energy, the best ligand is quercetin. Based on inhibition constant, the best inhibitor is also quercetin, followed by myricetin, then kaempferol as tested ligand. The statistical analysis also revealed the significant differences of molecular docking parameters between tested ligands and comparison ligand (**Figure 4**).

The MD simulation also revealed that all of tested ligands have a stable condition when they bind into the active sites of target proteins through RMSD, RMSF, Rg, and SASA parameters. Significant fluctuations in RMSD indicated instability, while minimal fluctuations suggested that the system has stabilized. The average value or the fluctuations of RMSD below 2.5 Å are acceptable for ligand-protein stable interaction. In contrast, fluctuations more than 3 Å indicate that the protein underwent a significant conformational change during the simulation, or that the protein is unstable [38]. Based on RMSD value the best tested ligand was quercetin for TGF-β1 and kaempferol for galectin-3. The high RMSF values were predicted to indicate weaker interactions and stability between the ligands and the receptor [37]. RMSF used to assess the stability and mobility of local proteins when the ligands bind to the target proteins, with the best RMSF value of tested ligand is quercetin for both TGF-β1 and galectin-3. While Rg is the indicator of stability and compactness of the structure, with quercetin is the best tested ligand for TGF-β1 and myricetin for galectin-3 through Rg analysis. SASA is used as a parameter to describe the protein solvent interactions ratio that predicts the degree of conformational changes in the binding processes and can be used to evaluate the protein accessibility. Overall, quercetin from tested ligand also had lower SASA which makes a compact and stable bond with TGF-β1, followed by myricetin and kaempferol as tested ligands, then colchicine as comparison ligand. Based on SASA value, quercetin was the best tested ligand for TGF-β1 and kaempferol for galectin-3. Overall, through the MD simulation the best tested ligand for TGF-β1 wass quercetin, followed by myricetin and kaempferol, while for galectin-3, the best tested ligand was myricetin followed by quercetin and kaempferol. Additionally, through the MMGBSA analysis quercetin was proven to be the best ligand for both TGF-β1 and galectin-3. Meanwhile, through the PCA based FEL analysis, the best tested ligand for both TGF-β1 and galectin-3 was quercetin. On the other hand, ADMET property showed that these agents did not violate any of Lipinsky's criteria, good pharmacokinetics profiles, and also had low toxicity to liver, heart rhythm, and non-carcinogenesis.

Nevertheless, the implications of the findings in the present study are not only limited for cardiac fibrosis since TGF-β1 and galectin-3, but it can also present in other tissue. Validation through in vitro or in vivo study is required to confirm the activity of the aforementioned drugs on cardiac fibrosis. Another limitation of this study includes its inability to explore further plant-based compounds which might have more potent activity.

## Conclusion

Findings from the in silico investigation in the present study suggested that quercetin, myricetin, and kaempferol exhibited strong binding affinities to the active sites of TGF-β1 and galectin-3, where stable and compact conformations of ligand-protein were observed. The results also indicated that these compounds may have favorable pharmacokinetic profiles and low predicted toxicity. However, further in vitro and in vivo studies are necessary to validate the potential of quercetin, myricetin, and kaempferol in inhibiting cardiac fibrosis before considering their evaluation in clinical trials.

### Ethics approval

Not required.

### Acknowledgments

None.

### Competing interests

All the authors declare that there are no conflicts of interest.

### Funding

This study received no external funding.

### Underlying data

Derived data supporting the findings of this study are available from the corresponding author on request.

### Declaration of artificial intelligence use

This study used artificial intelligence (AI) tools and methodologies for data analysis and modeling in the following capacities: machine learning algorithms, including molecular docking, molecular dynamic simulation, and ADMET analysis were used to analyze the dataset and predict outcomes. These analyses were implemented using AutoDock tools, BIOVIA Discovery Studio Visualizer 2021 tools, PyMol tools, CHARMM-GUI webserver (https://www.charmm-gui.org), NAMD software, VMD tools, OriginLab2018 tools, and ADMETlab 2.0 webserver (https://admetmesh.scbdd.com/service/evaluation/index). We confirm that all AI-assisted processes were critically reviewed by the authors to ensure the integrity and reliability of the results. The final decisions and interpretations presented in this article were solely made by the authors.

## How to cite

Suryono S, Amien MI, Tohari AI, *et al.* In silico studies on quercetin, myricetin, and kaempferol in inhibiting TGF-β1 and galectin-3 for cardiac fibrosis management. Narra J 2025; 5 (1): e1310 - http://doi.org/10.52225/narra.v5i1.1310.

## References

1. Gutierrez PS, de Campos FPF. Endomyocardial fibrosis. Autops Case Rep 2017;7:3-6.
2. Mocumbi AOH, Falase AO. Recent advances in the epidemiology, diagnosis and treatment of endomyocardial fibrosis in Africa. Heart 2013;99:1481-1487.
3. Flanigan MJ, Velez MR, Ruden EA, *et al.* Löffler endocarditis and endomyocardial fibrosis. J Am Osteopath Assoc 2017;117:601.
4. Low WCC, Hess CN, Hiatt WR, *et al.* Clinical update: Cardiovascular disease in diabetes mellitus: Atherosclerotic cardiovascular disease and heart failure in type 2 diabetes mellitus - Mechanisms, management, and clinical considerations. Circulation 2016;133:2459-2502.
5. Li Y, Li T, Zhou Z, *et al.* Emerging roles of Galectin-3 in diabetes and diabetes complications: A snapshot. Rev Endocr Metab Disord 2022;23:569-577.
6. Russo I, Frangogiannis NG. Diabetes-associated cardiac fibrosis: Cellular effectors, molecular mechanisms and therapeutic opportunities. J Mol Cell Cardiol 2016;90:84-93.
7. Khalil H, Kanisicak O, Prasad V, *et al.* Fibroblast-specific TGF-β–Smad2/3 signaling underlies cardiac fibrosis. J Clin Invest 2017;127:3770-3783.
8. Ma Z-G, Yuan Y-P, Wu H-M, *et al.* Cardiac fibrosis: New insights into the pathogenesis. Int J Biol Sci 2018;14:1645-1657.
9. Sharma UC, Mosleh W, Chaudhari MR, *et al.* Myocardial and serum galectin-3 expression dynamics marks post-myocardial infarction cardiac remodelling. Heart Lung Circ 2017;26:736-745.
10. Martínez-Martínez E, Brugnolaro C, Ibarrola J, *et al.* CT-1 (Cardiotrophin-1)-Gal-3 (Galectin-3) axis in cardiac fibrosis and inflammation. Hypertension 2019;73:602-611.

11. Suryono S, Rohman MS, Widjajanto E, *et al*. Effect of colchicine in reducing MMP-9, NOX2, and TGF- β1 after myocardial infarction. BMC Cardiovasc Disord 2023;23:449.
12. Suryono S, Rohman MS, Widjajanto E, *et al*. Colchicine as potential inhibitor targeting MMP-9, NOX2 and TGF-β1 in myocardial infarction: A combination of docking and molecular dynamic simulation study. J Biomol Struct Dyn 2023;41(21):12214-12224.
13. An Z, Yang G, Zheng H, *et al*. Biomarkers in patients with myocardial fibrosis. Open Life Sci 2017;12:337-344.
14. Walton KL, Johnson KE, Harrison CA. Targeting TGF-β mediated SMAD signaling for the prevention of fibrosis. Front Pharmacol 2017;8:461.
15. Parichatikanond W, Luangmonkong T, Mangmool S, *et al*. Therapeutic targets for the treatment of cardiac fibrosis and cancer: Focusing on TGF-β signaling. Front Cardiovasc Med 2020;7:34.
16. Yi M, Wei T, Wang Y, *et al*. The potassium channel KCa3.1 constitutes a pharmacological target for astrogliosis associated with ischemia stroke. J Neuroinflammation 2017;14(1):203.
17. Inoue R, Kurahara L-H, Hiraishi K. TRP channels in cardiac and intestinal fibrosis. Semin Cell Dev Biol 2019;94:40-49.
18. Davis J, Burr AR, Davis GF, et al. A TRPC6-dependent pathway for myofibroblast transdifferentiation and wound healing in vivo. Dev Cell. 2012;23:705–15.
19. Lin BL, Matera D, Doerner JF, *et al*. In vivo selective inhibition of TRPC6 by antagonist BI 749327 ameliorates fibrosis and dysfunction in cardiac and renal disease. Proc Natl Acad Sci USA 2019;116:10156–10161.
20. She G, Hou M-C, Zhang Y, *et al*. Gal-3 (Galectin-3) and KCa3.1 mediate heterogeneous cell coupling and myocardial fibrogenesis driven by βAR (β-Adrenoceptor) activation. Hypertension 2020;75:393-404.
21. Sygitowicz G, Maciejak-Jastrzębska A, Sitkiewicz D. The diagnostic and therapeutic potential of Galectin-3 in cardiovascular diseases. Biomolecules 2021;12:46.
22. Miean KH, Mohamed SJ. Flavonoid (myricetin, quercetin, kaempferol, luteolin, and apigenin) content of edible tropical plants. Agric Food Chem 2001;49:3106-3112.
23. Mahmud AR, EmaTI, Siddiquee MF, et al. Natural flavonols: Actions, mechanisms, and potential therapeutic utility for various diseases. Beni-Suef Univ J Basic Appl Sci 2023;12:47.
24. Kozłowska A, Szostak-Węgierek D. Targeting cardiovascular diseases by flavonols: An update. Nutrients 2022; 14(7):1439.
25. Chagas MDSS, Behrens MD, Moragas-Tellis CJ, *et al*. Flavonols and flavones as potential anti-Inflammatory, antioxidant, and antibacterial compounds. Oxid Med Cell Longev 2022;2022:9966750.
26. Wu Q, Liu H, Liao J, *et al*. Colchicine prevents atrial fibrillation promotion by inhibiting IL-1beta-induced IL-6 release and atrial fibrosis in the rat sterile pericarditis model. Biomed Pharmacother 2020;129:110384.
27. Zhang FS, He QZ, Qin CH, *et al*. Therapeutic potential of colchicine in cardiovascular medicine: A pharmacological review. Acta Pharmacol Sin 2022;43(9):2173-2190.
28. Astiawati T, Rohman MS, Wihastuti TA, *et al*. Antifibrotic effects of colchicine on 3T3 cell line ischemia to mitigate detrimental remodeling. J Pharm Pharmacogn Res 2024;12(2):296-302.
29. Lipinski CA. Lead- and drug-like compounds: The rule-of-five revolution. Drug Discov Today Technol 2004;1(4):337-41.
30. Kim S, Chen J, Cheng T, *et al*. PubChem 2023 update. Nucleic Acids Res 2023;51(D1):D1373-D1380.
31. Jo S, Kim T, Iyer VG, *et al*. CHARMM-GUI: A web-based graphical user interface for CHARMM. J Comput Chem 2008;29:1859-1865.
32. Phillips JC, Hardy DJ, Maia JDC, *et al*. Scalable molecular dynamics on CPU and GPU architectures with NAMD. J Chem Phys 2020;153:044130.33.
33. Hijazi M, Wilkins DM, Ceriotti M. Fast-forward Langevin dynamics with momentum flips. J Chem Phys 2018;148.
34. Case DA, Brozell S, Cerutti D, *et al*. AMBER 2018. San Francisco; University of California; 2018.
35. Moberly JG, Bernards MT, Waynant KV. Key features and updates for Origin 2018. J Cheminform 2018;10:5.
36. Xiong G, Wu Z, Yi J, *et al*. ADMETlab 2.0: An integrated online platform for accurate and comprehensive predictions of ADMET properties. Nucleic Acids Res 2021;49(W1):W5-W14.
37. Martínez L. Automatic identification of mobile and rigid substructures in molecular dynamics simulations and fractional structural fluctuation analysis. PLoS One 2015;10(3):e0119264.
38. Patel S, Brooks CL. CHARMM fluctuating charge force field for proteins: I parameterization and application to bulk organic liquid simulations. J Comput Chem 2004;25:1-15
39. RahmanFI, Zulfa PO, BeočaninA, *et al*. Targeting phosphoglycerate dehydrogenase enzyme using ginger compounds to suppress thyroid cancer progression. Narra X 2024;2(1):e112.
40. Zulkifli B, Fakri F, Odigie J, *et al*. Chemometric-empowered spectroscopic techniques in pharmaceutical fields: A bibliometric analysis and updated review. Narra X 2023;1(1):e80.